

Article

## The Effect of Bias Voltage and Gas Pressure on the Structure, Adhesion and Wear Behavior of Diamond Like Carbon (DLC) Coatings With Si Interlayers

Liam Ward <sup>1\*</sup>, Fabian Junge <sup>2</sup>, Andreas Lampka <sup>2</sup>, Mark Dobbertin <sup>2</sup>, Christoph Mewes <sup>2</sup> and Marion Wienecke <sup>2</sup>

<sup>1</sup> School of Civil, Environmental and Chemical Engineering, Royal Melbourne Institute of Technology, GPO Box 2476, Melbourne, Victoria 3001, Australia

<sup>2</sup> Institute of Surface and Thin Film Technology, Hochschule Wismar, PF 1210, 23952 Wismar, Germany; E-Mails: fabian.junge@thyssenkrupp.com (F.J.); andreas.lampka@hs-wismar.de (A.L.); marc.dobbertin@gmx.de (M.D.); christoph.mewes@hs-wismar.de (C.M.); marion.wienecke@hs-wismar.de (M.W.)

\* Author to whom correspondence should be addressed; E-Mail: liam.ward@rmit.edu.au; Tel.: +61-3-9925-1713; Fax: +61-3-9639-0168.

Received: 12 February 2014; in revised form: 21 March 2014 / Accepted: 24 March 2014 /

Published: 1 April 2014

---

**Abstract:** In this study diamond like carbon (DLC) coatings with Si interlayers were deposited on 316L stainless steel with varying gas pressure and substrate bias voltage using plasma enhanced chemical vapor deposition (PECVD) technology. Coating and interlayer thickness values were determined using X-ray photoelectron spectroscopy (XPS) which also revealed the presence of a gradient layer at the coating substrate interface. Coatings were evaluated in terms of the hardness, elastic modulus, wear behavior and adhesion. Deposition rate generally increased with increasing bias voltage and increasing gas pressure. At low working gas pressures, hardness and modulus of elasticity increased with increasing bias voltage. Reduced hardness and modulus of elasticity were observed at higher gas pressures. Increased adhesion was generally observed at lower bias voltages and higher gas pressures. All DLC coatings significantly improved the overall wear resistance of the base material. Lower wear rates were observed for coatings deposited with lower bias voltages. For coatings that showed wear tracks considerably deeper than the coating thickness but without spallation, the wear behavior was largely attributed to deformation of both the coating and substrate with some cracks at the wear track edges. This suggests that coatings deposited

under certain conditions can exhibit ultra high flexible properties.

**Keywords:** diamond like carbon (DLC); plasma enhanced chemical vapor deposition (PECVD); Si interlayer; XPS; elastic modulus; wear; hardness; adhesion

---

## 1. Introduction

The use of diamond like carbon (DLC) coatings has found widespread usage in many areas of engineering due to substantial benefits associated with properties including high surface hardness low friction, improved wear resistance, chemical inertness and enhanced corrosion resistance. One area of considerable interest is biomedical applications, particularly orthopaedic applications, such as knee and hip joint replacements [1,2] where these properties combined with excellent biocompatibility make them extremely attractive candidates. The tribological behavior of these coatings has been studied when deposited on a range of biomaterial substrates to include Co-Cr alloys [1,3–7], Ti alloys [8], stainless steels [9–11] and ultra high molecular weight polyethylene (UHMWPE) [12,13]. Significant reductions in the wear rates have been observed for DLC coated CoCr alloy in contact with UHMWPE [1,3,4] and CoCr alloy [6] compared with uncoated CoCr alloy which was observed to decrease with increasing film thickness [3,4]. This was attributed to increased surface roughness of the thicker coatings [3].

The presence of a DLC coating was observed to improve the wear resistance of 316L stainless steel [11]. Significant reductions in the wear rates of 316L stainless steel coated with DLC in sliding contact with DLC coated 316L stainless steel [10] and UHMWPE [9] have been reported to such an extent that the low level of wear observed was comparable to that for ceramic femoral heads [9]. Further, the effects of depositing multi-layered coatings systems [14] and the use of doped interlayers [15] have been studied with a view to optimising the wear behavior and adhesion.

While significant benefits have been achieved with these coatings in terms of improved hardness and wear resistance, problems associated with porosity and poor adhesion have limited their use in orthopaedic applications. A number of techniques including optimisation of the process parameters can reduce these limitations. In particular, one method of improving film to substrate adhesion has been through the deposition of interlayers, Si interlayers have been deposited to improve the adhesion of DLC on stainless steel [16,17], D2 steel [18], Ti alloys [19], and NiTi alloys [20]. Improved corrosion resistance [20,21] and reduced spalling [21] and friction [20] have also been associated with Si interlayers [21]. In contrast, DLC coatings deposited on Mg-Li alloys were observed to exhibit poor adhesion with a Si interlayer compared to DLC coatings deposited directly onto the substrate [22]. While Si interlayers were shown to improve the adhesion of DLC coatings on ceramic substrates, a Ti interlayer was observed to reduce the adhesion [23]. This was attributed to poor bonding between the Ti and DLC film.

Clearly, a number of distinct advantages in addition to film to substrate adhesion can be achieved through the deposition of a Si interlayer. The focus of this study was to systematically investigate the properties, particularly hardness, modulus of elasticity, adhesion, friction and wear behavior of plasma enhanced chemical vapor deposited (PECVD) DLC coatings deposited on 316L stainless steel substrates

with the addition of a Si interlayer, as a function of the substrate bias voltage and the system gas pressure.

## 2. Experimental Section

The surface of the 316L stainless steel samples, having dimensions 20 mm × 10 mm × 2 mm, were polished using standard metallographic preparation procedures, which involved successive grinding using various grade SiC papers and diamond paste polishing down to 0.25 μm finish. All samples were then subject to a chemical cleaning treatment using a three stage process; ultrasonic de-greasing for 5 minutes with trichloroethylene followed by cleaning in acetone and finally ultrasonic cleaning in ethanol for 5 minutes. Further details of standard cleaning procedures adopted in this study are available from the literature [24,25].

PECVD was used to deposit the DLC coatings. The system was initially pumped down to a vacuum of  $10^{-5}$  mbar, prior to backfilling with the reactant and inert gases ( $C_2H_2$ , HMDSO and Ar, respectively). Liquid Hexamethyldisiloxane (HMDSO) was contained in a reservoir connected to the vacuum chamber of the coating facility. At the working gas pressures employed in this study, the vapor pressure of HMDSO allows for vapourisation at room temperature, as the HMDSO is transferred to the vacuum chamber, although heating the liquid reservoir can facilitate this process. The plasma was generated using an HF generator which applied a high-frequency voltage on the anode. Atomic cleaning of the sample surface was conducted using a plasma etch treatment, an integral part of the PECVD chamber, prior to depositing the DLC coatings. The applied plasma etch parameters were 100 W power, 30 sccm argon flow, an etch time of 15 min and a gas pressure of 30 μbar.

After sputter cleaning, the Si interlayer was deposited for 2 min using HMDSO as the silicon precursor under the following conditions; bias voltage 300 V; gas pressure 15 μbar; argon flow rate 30 sccm. Following this, DLC coatings were deposited with combined parameter variations of substrate bias voltage (250, 300 and 350 V) and gas pressure (5, 10 and 15 μbar).  $C_2H_2$  gas flow was maintained at 30 sccm. The deposition time for all coatings was maintained at 45 minutes. Sample identification and corresponding process variables are shown in Table 1.

**Table 1.** Sample identification, process variables, deposition rates, coating and transition layer thicknesses for diamond like carbon (DLC) coatings deposited with Si interlayers at varying bias voltage and gas pressure.

Sample	Pressure [μbar]	Bias Voltage [V]	Coating Thickness [μm]	Deposition Rate [nm/min]	Silicon Layer Thickness [μm]
DLC-Si-316L-01		250	1.9	42	0.2
DLC-Si-316L-02	5	300	2.5	60	0.2
DLC-Si-316L-03		350	3.0	67	0.2
DLC-Si-316L-04		250	2.2	49	0.2
DLC-Si-316L-05	10	300	1.3	29	0.2
DLC-Si-316L-06		350	4.0	89	0.3
DLC-Si-316L-07		250	3.6	80	0.3
DLC-Si-316L-08	15	300	4.3	96	N/A
DLC-Si-316L-09		350	5.3	118	N/A

In order to determine the DLC coating thickness X-ray photoelectron spectroscopy (XPS) depth profiles were performed. C, Fe and O were analysed at various levels after the surface composition was measured initially. This was achieved by successive argon sputter etching. A standard etching rate of 0.2 nm/s was chosen. The ion gun energy for sputtering was set at 3000 eV. After etching, the surface composition was measured again. This procedure was repeated for 10–90 levels, depending on the coating thickness. Examination of the concentration profiles not only provides an indication of the coating thickness, but also the chemical composition in the interlayer.

Bonding states ( $sp^2/sp^3$ ) were measured in the first nine (etched) levels of the depth profile to provide an accurate indication of the coating composition with averaged values. The range of the  $sp^2$  binding energy peak was found to be between 284.24 and 285.3 eV which led to an average value of  $284.6 \pm 0.32$  eV. Using the value fitting software, 284.55 eV was chosen. Similarly, the range of the  $sp^3$  binding energy peak was found to be between 284.5 and 285.9 eV which led to an average value of  $285.32 \pm 0.32$  eV. Using the value fitting software, 85.55 eV was chosen.

Structural and morphological features of the DLC coatings were analysed using transmission electron microscopy (TEM) studies. Freestanding carbon films with thickness less than 200 nm were prepared by the deposition of DLC films on NaCl single crystal substrates under the same process conditions of the current investigation. After dissolving the NaCl substrates, the freestanding films were transferred from the solution directly onto TEM grids for analysis in the TEM.

Hardness and modulus of elasticity measurements were performed using a MTS nano-indenter xp (Surface Systems + Technology GmbH & Co, Hückelhoven, Germany) with a three-sided pyramidal diamond (Berkovich) tip in csm (continuous stiffness measurement) mode. Scan speed was 1 nm/s. For each sample, 49 indents were utilised ( $7 \times 7$  matrix at 10  $\mu\text{m}$  spacing between indents) to calculate the average hardness and elastic modulus values and associated standard deviations. To prevent any influence from the substrate, readings were obtained from depth displacements of no greater than 10% of the coating thickness. Hardness and elastic modulus values were generated directly using NanoSuite 5 software [26] with load, displacement and stiffness as the input variables. Here,  $E$  and  $H$  were determined from load displacement ( $P$ - $h$ ) curves over a range of indenter penetrations. A sharp, fixed-profile indenter is pressed onto the top surface at load  $P$ , with characteristic maximum penetration depth  $h$ . From the load–displacement curve generated, three important parameters the maximum load,  $P_{\text{max}}$ , maximum depth,  $h_{\text{max}}$ , and stiffness,  $S$  (where  $S = dP/dh$ ) are calculated. Once the contact area,  $A$ , is known, the hardness  $H$ , can be calculated from the following equation:

$$H = P_{\text{max}} / A \quad (1)$$

The reduced modulus of elasticity,  $E_r$ , is calculated from the following equation, using knowledge of the contact area and measured unloading stiffness:

$$E_r = \left(\frac{1}{\beta}\right) \cdot \left(\frac{\sqrt{\pi}}{2}\right) \cdot \frac{S}{\sqrt{A}} \quad (2)$$

where  $\beta$  is a dimensionless parameter normally taken as unity. A detailed account of measuring hardness and modulus of elasticity has been described elsewhere [27].

Wear tests were conducted at ambient temperature (22 °C) and 51% relative humidity using a CSEM Tribometer (pin-on-disc). All tests were conducted using a 6 mm diameter ruby ball in contact with the coated steel surface under an applied load of 20 N. The tracking speed and sliding distance were held

constant at  $0.3 \text{ ms}^{-1}$  and 500 m respectively. The lubricant used was ethanol. Wear track profiles were measured using a KLA Tencor Alpha-Step IQ surface profilometer (KLA-Tencor, Milpitas, CA, USA). Wear volumes generated were calculated from the wear track profile using an Excel model. Analysis of the wear tracks were carried out using SEM, EDS and XPS.

The contact stresses based upon the ball configuration and material were calculated from Equation 3 and were found to be in the range 0.9–1.1 GPa for all samples tested.

$$P_{\max} = 0.38 [F_N E^2 / R^2]^{1/3} \quad (3)$$

where  $F_N$  is the load (20 N),  $E$  is the measured Elastic Modulus (157–217.8 GPa range) and  $R$  is the radius of the ball (0.006 m).

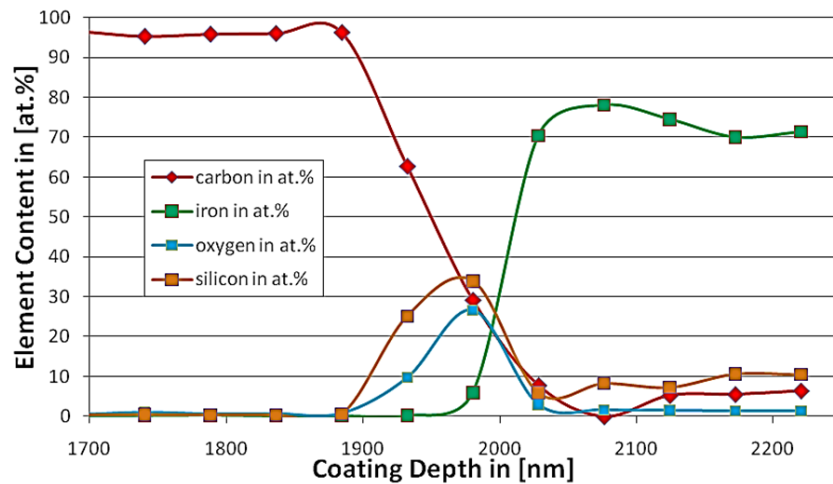
In order to assess the adhesion qualitatively, with respect to the parameter variation, all coated samples were scratch tested with a diamond tip and a constant applied load of 0.5 N. After testing, the scratch channels were examined using optical microscopy (images recorded at a magnification of 500 times) for the various failure modes within and outside the scratch channel.

### 3. Results

#### 3.1. XPS Depth Profiling Analysis for Coating Thickness Measurements

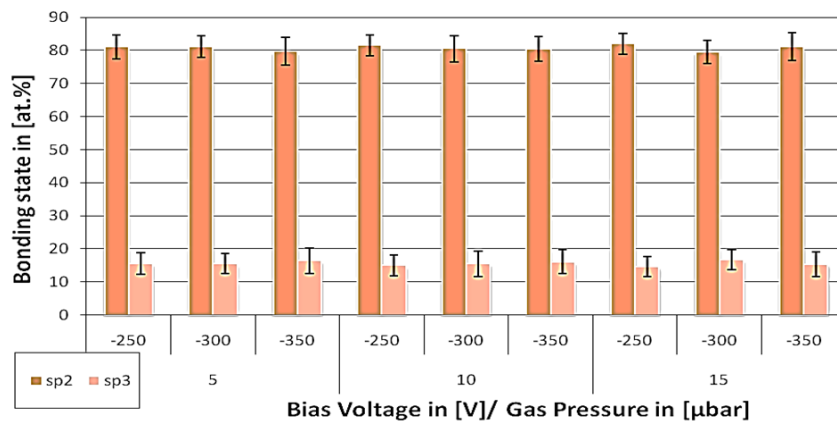
Figure 1 shows a typical XPS depth profile for sample DLC-Si-316L-01. Analysis of the profile yields some very important information, regarding the coating, the substrate and a graded interlayer. Firstly, the presence of the DLC coating and the coating thickness can be calculated from the profile. The thickness of the DLC coating can be determined by profile distance, when the carbon content is a constant maximum (~98%) and the Fe content is zero. Likewise the pure steel substrate is evidenced by a profile indicating the presence of almost 0%–5% C and 70%–80% Fe. Secondly the presence of a diffusion layer, the thickness calculated from the distance over which the gradual reduction in the C concentration from 98% to approx. 0%–5% occurs with the corresponding increase in the Fe concentration from 0% to 70%–80%. Thirdly, the presence of the Si interlayer, indicated by the Si and O profiles, showing the corresponding increase and decrease in content of both atomic species, over a distance corresponding to the diffuse region. It is thought that the simultaneous presence of Si and O is associated with silicon precursor gas Hexamethyldisiloxane (HMDSO) which also contains oxygen and Carbon ( $\text{Si}_2\text{OC}_6\text{H}_{18}$ ). Subsequent analysis of all other coatings considered and analysis of the data enabled calculation of the coating thickness and gradient layer containing Si as shown in Table 1. It should be noted that this method of calculating thickness of the coating and Si interlayer thickness provides only approximate values and the figures provided in Table 1 may have deviations, typically up to +/-5%.

The coating thickness varied, depending on the process deposition parameters, in the range of ~1.3–5.3  $\mu\text{m}$ . A general observation is that coating thickness increases with increasing gas pressure at any given bias voltage and increasing bias voltage at any given gas pressure. This maximum coating thickness of ~5.3  $\mu\text{m}$  was achieved for the DLC-Si-316L-09 coating with the highest gas pressure and highest bias voltage (15  $\mu\text{bar}$  and 350 V). Deposition rates as shown in Table 1, varied proportionally with film thickness, yielding rates varying from 29 to 118 nm/min, as the deposition time was maintained constant for all coatings considered.

**Figure 1.** X-ray photoelectron spectroscopy (XPS) depth profile for sample DLC-Si-316L-01.

### 3.2. Determination of Chemical Bonding States ( $sp^2/sp^3$ Contents) from XPS

Figure 2 shows the  $sp^2$  and  $sp^3$  content for samples DLC-Si-316L-01 to -09 which were deposited at various bias voltage and gas pressures. All  $sp^2$  and  $sp^3$  amounts were observed to lie between 79.6–82 at% for  $sp^2$  and 15–6.7 at% for  $sp^3$ . No observable trends (decreasing or increasing  $sp^2/sp^3$  amounts) were observed with changing bias voltage or gas pressure.

**Figure 2.** Chemical bonding states ( $sp^2/sp^3$  content) for samples DLC-Si-316L-01 to DLC-Si-316L-09.

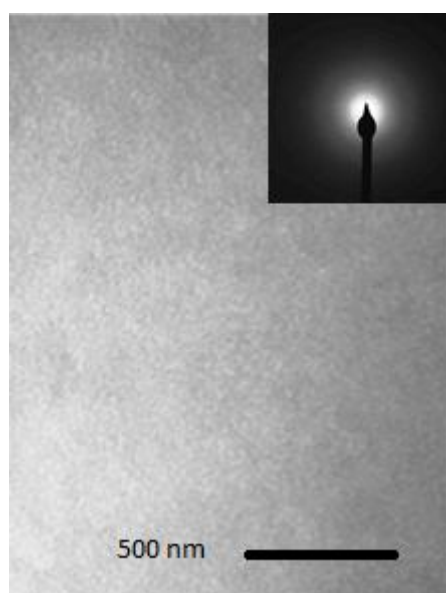
### 3.3. Structure, Hardness and Modulus of Elasticity Results

Figure 3 shows a typical TEM image and corresponding selective area electron diffraction pattern (SAED) for the DLC coatings deposited in this study. The dense, featureless images observed combined with the absence of any diffraction rings confirm that these DLC carbon films showed no crystalline microstructure and were indeed completely amorphous.

Table 2 shows the hardness and modulus of elasticity results for the DLC coated samples as a function of gas pressure and bias voltage (DLC-Si-316L-01 to DLC-Si-316L-09), compared with uncoated 316L stainless steel as a reference. In general, the deposition of DLC led to a significant

increase in hardness from 2.9 GPa to values ranging from 19.1 to 27.3 GPa. While the modulus of elasticity decreased in most cases from 220.4 GPa down to values typically in the range 157–206 GPa. Hardness and modulus of elasticity increased with increasing bias voltage at the low gas pressures, while at higher gas pressures, no such correlations were observed. Increased  $C_2H_2$  gas pressure generally induced a decrease in the hardness and modulus of elasticity at a given bias voltage.

**Figure 3.** Transmission electron micrograph (TEM) image and corresponding selective area electron diffraction pattern (SAED) for a typical diamond like carbon (DLC) coating deposited in this study.



**Table 2.** Hardness and modulus of elasticity values for DLC coatings DLC-Si-316L-01 to DLC-Si-316L-09.

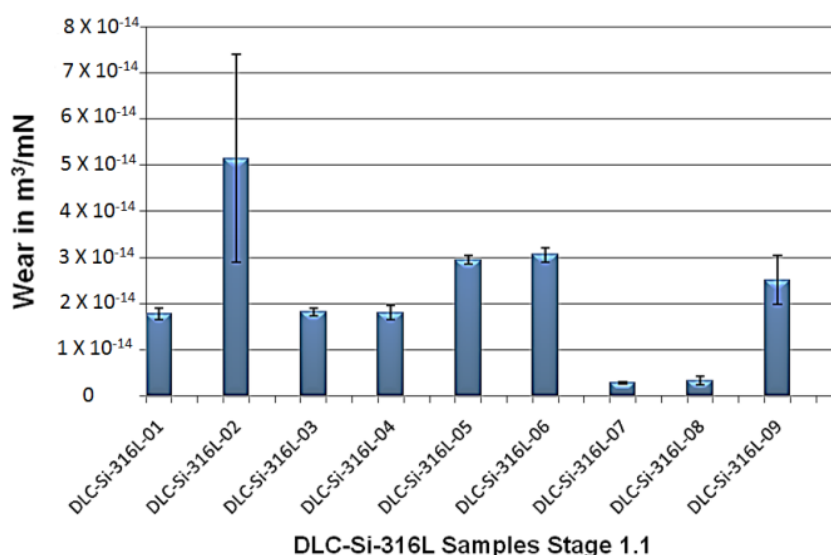
Sample	Hardness [GPa]	Standard Deviation [GPa]	Modulus of Elasticity [GPa]	Standard Deviation [GPa]
Uncoated 316L	2.9	0.2	220.4	12.9
DLC-Si-316L-01	25.4	1.5	190.5	7
DLC-Si-316L-02	25.6	1.3	206.6	5.6
DLC-Si-316L-03	27.3	1.7	217.8	8.5
DLC-Si-316L-04	20.6	1.2	158.9	5.4
DLC-Si-316L-05	20.6	1.2	170.5	6.3
DLC-Si-316L-06	20.3	1.3	159.6	5.8
DLC-Si-316L-09	19.0	1.1	157	6.1

Analysis of the hardness and elastic modulus data as a function of coating thickness shows conflicting results. Hardness and elastic modulus were observed to increase with increasing coating thickness as a result of bias voltage increases (constant gas pressure). However, a decrease in the hardness and elastic modulus was observed with increasing coating thickness as a result of increasing gas pressure (constant bias voltage). These results highlight the complex interactions associated with the process deposition variables and the resultant effects on the properties.

### 3.4. Wear Test Results

The wear test results showing the wear volume removed from the coatings are shown in Figure 4. The deposition of the DLC coatings led to a significant improvement in the overall wear resistance, the wear rate for the uncoated 316L sample was  $3.38 \times 10^{-12} \text{ m}^3/\text{mN}$  (not shown in Figure 3) in contrast to the lowest wear rate value of  $2.8 \times 10^{-15} \text{ m}^3/\text{mN}$  for sample DLC-Si-316L-07. These results indicate that the wear rate could be reduced by factors ranging from  $\sim 65$  (DLC-Si-316L-02) to  $\sim 1200$  (DLC-Si-316L-07) depending on the process parameters.

**Figure 4.** Variation in wear rates for DLC coatings with Si interlayers at varying bias voltage and gas pressure.

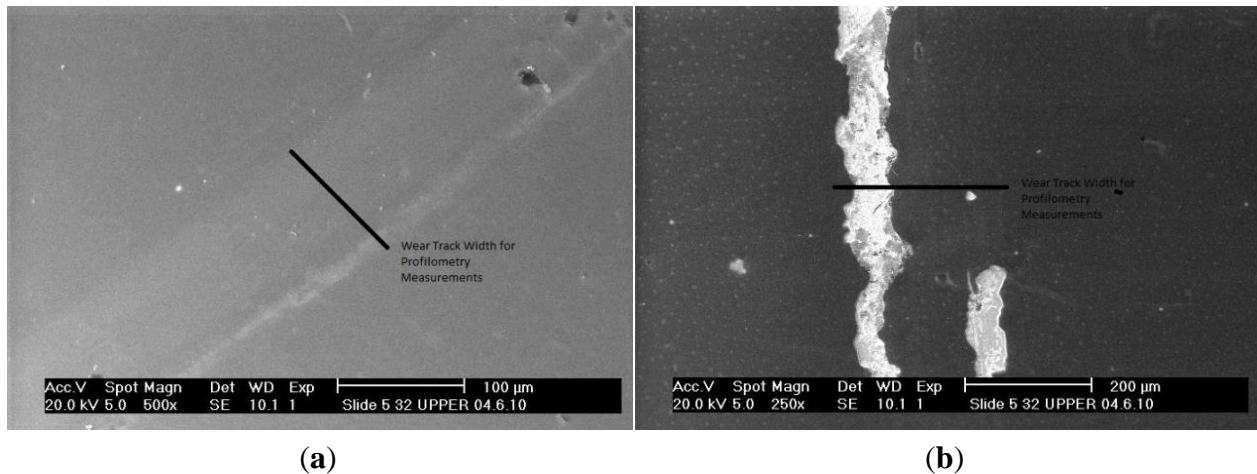


Generally, at the intermediate to high gas pressures (10 and 15  $\mu\text{bar}$ ), wear resistance was observed to decrease (higher wear rates) with increasing bias voltage. It is interesting to note that coating DLC-Si-316L-02 not only showed the highest wear rate but also exhibited the largest deviation from all samples investigated. This could be associated with inconsistent wear/deformation within the wear track, supporting the need for measuring a number of wear profiles within the wear track to obtain a statistically viable result.

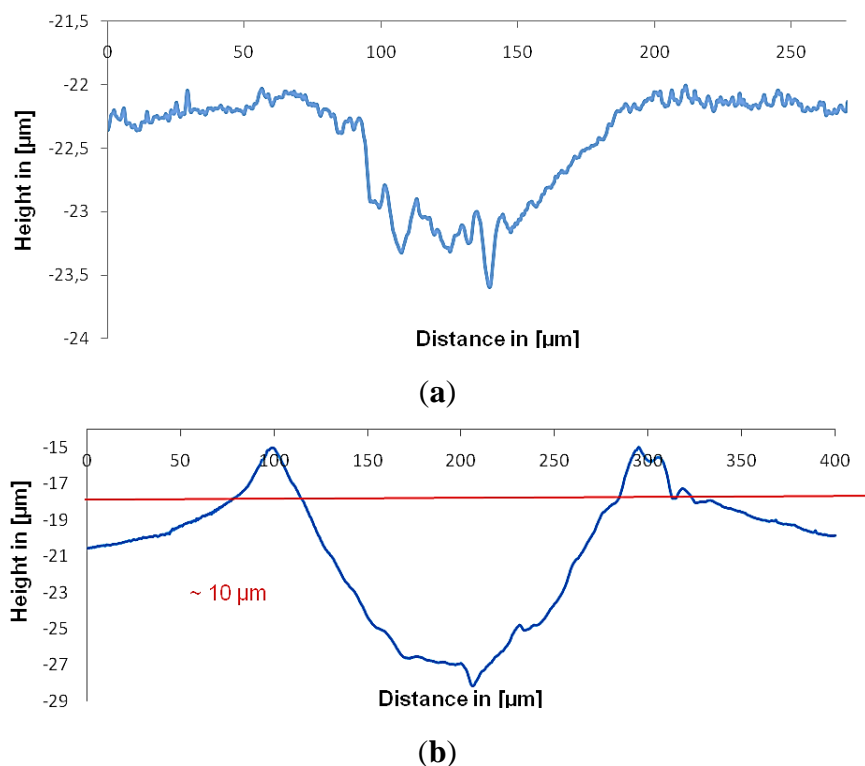
SEM micrographs of coatings with low (DLC-Si-316L-07) and high (DLC-Si-316L-06) wear rates are shown in Figure 5a,b respectively. The more wear resistant coating DLC-Si-316L-07 has a wear track showing slight deformation and possibly some cracking, but no coating removal (Figure 5a) in contrast to coating DLC-Si-316L-06 (Figure 5b) showing cracking and coating spallation over a significant area of the wear track, particularly at the edges of the wear track.

Figure 6a shows a representative wear track profile taken from sample DLC-Si-316L-07. The wear track profiles exhibited a depth of approximately 1.5  $\mu\text{m}$  which is significantly lower than the coating thickness of  $\sim 3.6 \mu\text{m}$ . In contrast, the wear track profile taken from sample DLC-Si-316L-06 (Figure 6b) has a depth of approximately 10  $\mu\text{m}$ , which is significantly higher than the coating thickness of  $\sim 4.0 \mu\text{m}$ .

**Figure 5.** (a) SEM of DLC coating DLC-Si-316L-07 wear track (500× Magnification); (b) SEM of DLC coating DLC-Si-316L-06 wear track (250× Magnification).



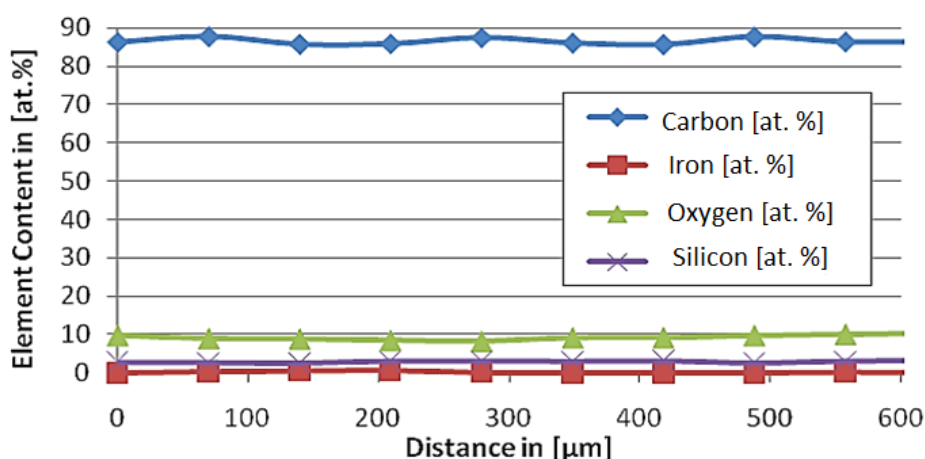
**Figure 6.** (a) Wear track profile from coating DLC-Si-316L-07; (b) Wear track profile from coating DLC-Si-316L-06.



A XPS scan of the wear track of sample DLC-Si-316L-07 (Figure 7) shows a homogeneous distribution of elements C (approx. 90%) and O (approx. 10%) with no Fe or Si present, indicating that the coating is present over most of the wear track surface, confirming no removal of the coating after wear testing. For sample DLC-Si-316L-06, the wear track depth exceeded the coating depth by a factor of approx. 2.5 times at the centre of the wear track, inferring that all the coating should have been removed (particularly at the centre) if the wear track depth is associated purely with wear. However, the SEM image in Figure 5a, showing coating removal along the edges of the wear track and not in the centre confirms that the wear tracks generated are predominantly attributed to deformation of both the

coating and softer substrate system, and to a lesser extent, due to wear of the coating and subsequent wear of the substrate itself. For sample DLC-Si-316L-07 any wear is confined to the coating itself and the overall low wear characteristics are associated with both resistance to wear from the coating and resistance to deformation from the combined coating and substrate system. For sample DLC-Si-316L-06 which was 6–7 times deeper, the overall wear characteristics can be attributed predominantly to significantly increased deformation of the coating and substrate regions, and to a lesser extent wear of the coating itself. However, cracking and spallation of the coating was observed in this coating, although this was more likely to be associated with heavy substrate deformation resulting in the “egg shell” effect when subject to high contact stresses, particularly noticeable at the edges of the wear track where stresses are considerably higher. It would appear that the wear resistance of the coating system at lower bias voltages can be attributed to not only inherent improved wear resistance itself but also to inducing a resistance to plastic deformation when subject to sliding wear under high contact stresses.

**Figure 7.** XPS scan of wear track profile of coating DLC-Si-316L-06.



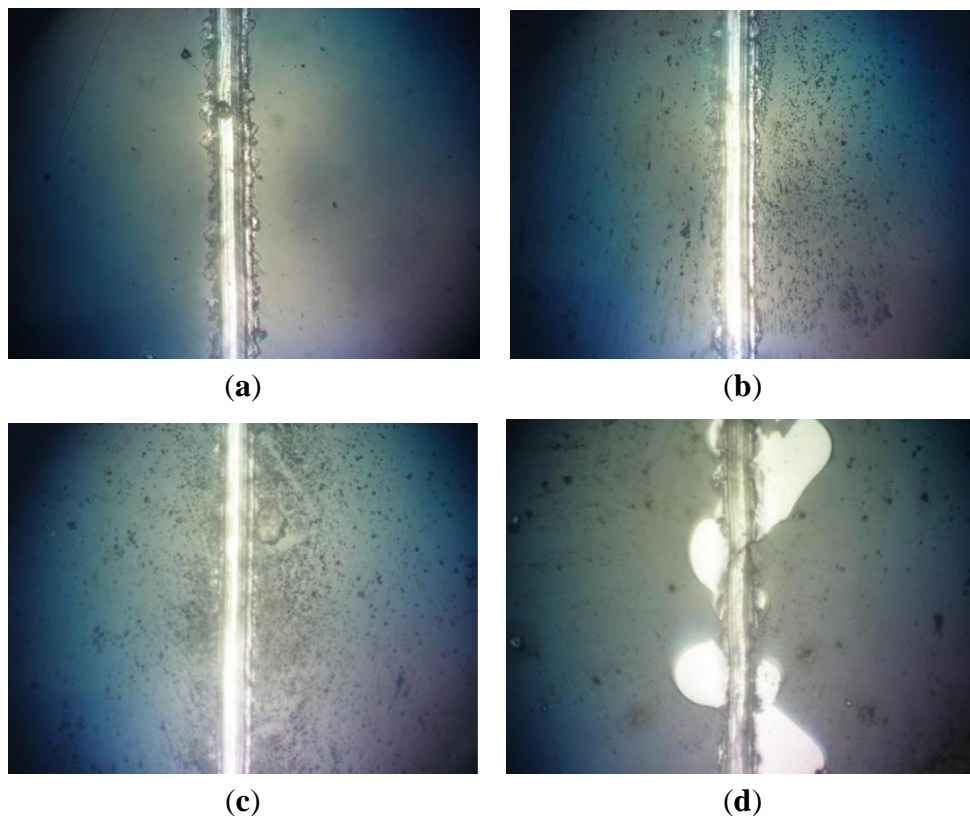
It should be noted that the theory postulated above regarding wear and deformation of the coating and substrate, would suggest that the substrate of coating DLC-Si-316L-06 deformed considerably more than that of coating DLC-Si-316L-07. While, the DLC coating itself may play a role in providing resistance to deformation for coating DLC-Si-316L-07, it is possible that the deposition conditions for coating DLC-Si-316L-06 (increased bias voltage) may have induced substrate softening. However, confirmation of this would require further work in this area. Nevertheless, the findings from this component of the study provide conclusive evidence that support the author’s belief that these DLC coatings with ultra-high flexible properties can be achieved with an appropriate coating system and optimal choice of deposition process parameters (low bias voltage of 250 V and high gas pressure of 15 μbar) and deposition conditions as indicated in the Experimental Section.

### 3.5. Adhesion (Scratch Test) Results

Optical micrographs of selected scratch channels conducted on DLC coatings with Si interlayers at varying bias voltage and gas pressure are shown in Figure 8a,b. All samples show quite good adhesion of the coating, since low spallations appear as shown for example in Figure 8a (sample DLC-Si-316L-04) and Figure 8b (sample DLC-Si-316L-06), even if sample DLC-Si-316L-06 is grown with a thickness of

4.4  $\mu\text{m}$  and has almost double the thickness of sample DLC-Si-316L-04 (2.2  $\mu\text{m}$ ). At higher bias voltage of 350 V (sample DLC-Si-316L-06, Figure 8b) a little more spallation at the wear track edges appears. For comparison, scratch test results are shown for samples grown under similar conditions but without Si-interlayer from unpublished work in Figure 8c,d. Figure 8c shows DLC-316L-01 (5  $\mu\text{bar}$ ,  $-250$  V, 2.2  $\mu\text{m}$ ) and Figure 8d shows DLC-316L-09 (15  $\mu\text{bar}$ ,  $-350$  V, 4.1  $\mu\text{m}$ ). The samples have similar hardness and elasticity, but the higher thickness seems to result in spallation. These results reveal that the Si interlayer improves adhesion of the carbon coating.

**Figure 8.** (a) Scratch test on sample DLC-Si-316L-04 at 0.5 N load and 500 $\times$ Magnification; (b) Scratch test on sample DLC-Si-316L-06 at 0.5 N load and 500 $\times$  Magnification; (c) Scratch test on sample DLC-316L-01 at 0.5 N load and 500 $\times$ Magnification; (d) Scratch test on sample DLC-316L-09 at 0.5 N load and 500 $\times$ Magnification.



## 4. Discussion

### 4.1. Influence of Process Parameters on Deposition Rate and Film Thickness

The DLC coating thickness was observed to vary with the working gas pressure and substrate bias voltage. As the deposition time was kept constant, the results would suggest that the deposition rate increased with increasing voltage and gas pressures. Deposition rates typically varied from 42.2 nm/min at 250 V bias and 5  $\mu\text{bar}$ , to 117.8 nm/min at 350 V bias and 15  $\mu\text{bar}$  gas pressure. A similar study conducted by Heeg *et al.* [27] revealed an increase in the deposition rate from 10 nm/min to over 90 nm/min was observed for PECVD DLC deposited on Ge substrates as the self-bias was increased from 200 to 400 V. Above 400 V, growth rate saturation was reached. From the current study, the

observed increase in deposition rate with increasing bias voltage is in agreement with the findings of Heeg *et al.* [28]. However, a saturation point was not reached, possibly due to the upper point of the bias voltage range considered being lower than 400 V. It is quite likely that increased deposition rate with both increasing bias voltage and increasing gas pressure can be explained firstly in terms of the energies of the arriving species at the substrate surface or the growing film, respectively, due to the acceleration by the electric field and secondly in terms of higher carbon feed in the gas phase at higher working pressure: Higher deposition rates can be attributed to increased attraction of ionised species to the substrates and growing films with higher bias. In addition, the arrival of species at the substrate surface with greater energies due to higher bias can result in improved adhesion and bonding of the coating species, thus reducing the formation of loosely bonded species which can be subsequently removed by re-sputtering.

The increase in deposition rate with gas pressure can be explained in terms of the energy of the arriving species arriving at the surface too. Studies conducted by Ward on sputtered Nb coatings and the effect of bias voltage and argon gas pressure [29] revealed that lower argon gas pressures induced more intense ion bombardment. Ions/neutrals arriving at the surface would maintain higher kinetic energies due to the virtually collision free paths they travel across the plasma at low working gas pressures and thus induce higher re-sputtering rates of loosely bonded adatoms at the coating surface and therefore suppressing film growth. At higher working gas pressures, ionic species arrive at the surface with reduced kinetic energies associated with lower mean collision free paths. This combined with increased gas scattering effects may have resulted in reduced re-sputtering effects. Another possibility is the higher gas pressures can increase the ionization efficiency of the plasma and hence ionized or partially ionized coating species arrive at the surface available for nucleation and growth of the coating.

The above discussion has focused on possible explanations for increased deposition rates/film thickness in terms of the ionization energies available as a result of variations in both bias voltage and gas pressure. It is likely that all these mechanisms have played a significant role in influencing the deposition rate as deposition rate increased (i) with increasing bias voltage at constant gas pressure and (ii) increasing gas pressure at constant bias voltage. However, it is not possible to state as to the extent that these mechanisms have contributed to the overall energy ionization.

#### 4.2. Influence of Process Parameters on Hardness and Modulus of Elasticity

The observed hardness and elastic modulus results are typical of those recorded in the literature [6,30,31] where the hardness of a-C:H coatings is within the range 18–40 GPa while the values for the modulus of elasticity are in the range of 25 to >400 GPa. Wu *et al.* [32] observed a reduction in DLC film hardness with increasing gas pressure. This was attributed to decreased ion energy due to collision phenomena thus producing ions with lower energy that make more graphitic carbon links and hence a coating with overall reduced hardness.

The influence of the coating parameters on hardness and Young's modulus values in terms of the ion bombardment energy, can be explained using the subplantation model of Robertson [33]. Initially, the carbon atoms from the PECVD plasma deposition have  $sp^2$  bonding states, which is at the lower-energy state. However due to the plasma conditions, a number of the carbon ions with a higher energy level penetrate the growing film (subplantation) and start to compact it which leads to formation of  $sp^3$

bondings and thus increases the density and energy in the growing amorphous film. Thus, increased bias voltage and reduced working gas pressures are expected to promote the formation of  $sp^3$  bonding, due to higher energy states of the carbon ions. In the current study, although  $sp^3$  bonding was observed in all the coatings, as shown in Figure 2, no correlations could be observed between chemical bonding states ( $sp^2/sp^3$  content) and changing bias voltage or gas pressure.

It is suggested that in the current study, increased ion energy for coatings deposited using higher bias voltages and lower gas pressures, due to mechanisms detailed in Section 4.1, may be responsible for the increased hardness and elastic modulus. While this has been associated with increased formation of  $sp^3$  bonding in the growing amorphous films [33], such correlations were not observed in the present study. However the energy of the accelerated ions is also dissipated through thermal process and relaxation. Therefore, the  $sp^3$  content attains a maximum value with increasing bias voltage, above which a further increase in the bias voltage results in decreasing  $sp^3$  content in the amorphous films.

It is further postulated that atoms arriving at the coating surface with greater energy due to longer mean free path at reduced gas pressure and higher bias voltages, due to greater acceleration of ionic species, may result in the generation of higher inherent stresses and localised strain fields set up in the coating, resulting in increased hardness and elastic modulus. However, residual stress analysis would need to be carried out to confirm the existence of any such correlations.

#### *4.3. Influence of Process Parameters on Wear and Adhesion Characteristics*

Analysis of the wear behavior and adhesion suggest that while both the bias voltage and working gas pressure influence the wear and adhesion characteristics of the coating, the bias voltage appears to be the more dominant factor in wear and adhesion behavior, more so than the gas pressure. In addition, there appears to be a correlation with the deposition rates. It is suggested that the improved adhesion at lower bias voltages, irrespective of the gas pressure, is associated with the production of thinner DLC films. This may be linked with lower internal stresses existing in the thinner coatings deposited at lower bias voltages. As mentioned in Section 4.2, residual stress analysis would need to be carried out to confirm the existence of any such correlations. Further, improved wear resistance for coatings with lower film thickness (deposited at lower bias voltage) may be attributed to combinations of improved adhesion and lower internal stresses within the system.

The increased wear resistance of the coatings observed in general at the higher gas pressures may be associated with the lower observed hardness and elastic modulus under such conditions, thus allowing the coatings to deform under high contact stresses rather than crack if too brittle.

#### *4.4. Influence of Si Interlayers on the Adhesion and Wear Behavior*

As shown in Section 3.4, the adhesion PECVD coatings without the presence of a Si interlayer showed that under the same deposition conditions (identical bias voltage/gas pressure combinations), reduced adhesion was observed at the higher bias voltages and gas pressures, however the cracking and spallation was more severe for the DLC coatings without a Si interlayer. At high bias voltage (350 V) and working gas pressure (15  $\mu$ bar) combinations, extensive regions where the coating has cracked and spalled away can be observed outside of the scratch track, as opposed to confined spallation at the edge of the scratch channel, in the presence of a Si interlayer (Figure 7b). These findings confirm that the

presence of a Si interlayer improves the adhesion characteristics, particularly at the higher bias voltage and gas pressure combinations. Furthermore, the adhesion of the DLC film to the substrate was so low that the film completely spalled off during the wear test.

In contrast, the observed wear rates were generally lower for all DLC coatings deposited at all bias voltages (250–350 V) and low to intermediate gas pressures (5–10  $\mu\text{bar}$ ) without the presence of a Si layer. Here, wear rates were typically in the range  $10^{-15}$   $\text{m}^3/\text{mN}$  and no more than  $1.0 \times 10^{-14}$   $\text{m}^3/\text{mN}$ . However at higher gas pressures, the wear rates were lowered in the presence of a Si interlayer.

## 5. Conclusions

XPS in depth profiling mode was used successfully to monitor the thickness of the DLC coating and thickness of any transient layer. Coating thickness generally increased with increasing bias voltage and increasing gas pressure. This was attributed to increased attraction of ionised species/high energy neutrals to the substrates/growing films with higher bias and increased ionization efficiency of the plasma at higher gas pressures.

All DLC coatings showed higher hardness than the uncoated samples. The hardness and modulus of elasticity were influenced predominantly by variations in the deposition process variables, and to a lesser extent by the coating thickness alone. At low working gas pressures, hardness and modulus of elasticity increased with increasing bias voltage. Reduced hardness and modulus of elasticity were observed with increasing gas pressures. This was possibly associated with decreased ion energy due to collision phenomena encouraging the formation of more graphitic carbon links.

Wear resistance improved significantly for all coating systems studied compared with the uncoated material. The wear resistance increased by a factor as high as  $\sim 1200\times$  when compared with the uncoated 316L. Lower wear rates were generally observed for thinner coatings deposited at intermediate to high gas pressures and lower bias voltages.

Increased adhesion was generally observed at lower bias voltages and higher gas pressures. This was attributed to thinner DLC films and the generation of lower internal stresses within the coating at lower bias voltages and lower hardness/elastic modulus at higher working gas.

The wear behavior of these coatings was largely attributed to deformation of both the coating and substrate with some coating removal at the wear track edges. This suggests that coatings deposited under certain conditions (low bias voltage and high working gas pressure) can exhibit ultra high flexible properties.

## 6. Future Work

To conduct residual stress analysis on DLC coatings with Si interlayers as a function of the applied bias voltage and working gas pressure.

To conduct similar adhesion, wear, hardness studies on DLC coatings with incorporation of various dopants (H, Ar, N, O, *etc.*) and multi-layered coating systems to further optimise the coating properties.

To assess the tribological properties of DLC coated 316L stainless steel in contact with alternative ceramic and steel counter material.

To conduct further wear tests under lubricating conditions and electrochemical corrosion studies in saline environments.

## Acknowledgments

The authors would like to acknowledge financial support in the form of internal staff development travel funding (School of Civil, Environmental and Chemical Engineering, RMIT University) and School funding from both RMIT Australia and Hochschule Wismar for support of a six month Masters Student Exchange Program initiative between the two institutes.

## Author Contributions

Preparation of the manuscript, final analysis and interpretation of the results conducted by Liam Ward and Marion Wienecke. Wear testing, XPS analysis, electron microscopy and generation of initial results conducted by Fabian Junge. Sample preparation, coating deposition, Nano indentation studies and adhesion scratch test studies conducted by Andreas Lampka, Mark Dobbertin and Christoph Mewes.

## Conflicts of Interest

The authors declare no conflict of interest.

## References

1. Dearnaley, G.; Arps, J. Biomedical applications of diamond-like carbon (DLC) coatings: A review. *Surf. Coat. Technol.* **2005**, *200*, 2518–2524.
2. Hauert, R. A review of modified DLC coatings for biological applications. *Diamond Relat. Mater.* **2003**, *12*, 583–589.
3. Thorwarth, G.; Falub, C.; Müller, U.; Weisse, B.; Voisard, C.; Tobler, M.; Hauert, R. Tribological behavior of DLC-coated articulating joint implants. *Acta Biomater.* **2010**, *6*, 2335–2341.
4. Reisel, A.; Schürer, C.; Müller, E. The wear resistance of diamond-like carbon coated and uncoated Co28Cr6Mo knee prostheses, *Diamond Relat. Mater.* **2004**, *13*, 823–827.
5. Saikko, V.; Ahlroos, T.; Calonius, O.; Kreänen, J. Wear simulation of total hip prostheses with polyethylene against CoCr, alumina and diamond-like carbon. *Biomaterials* **2001**, *22*, 1507–1514.
6. Sheeja, D.; Tay, B.; Nung, L. Feasibility of diamond-like carbon coatings for orthopaedic applications. *Diamond Relat. Mater.* **2004**, *13*, 184–190.
7. Galvin, A.; Brockett, C.; Hatto, P.; Burton, A.; Isaac, G.; Stone, M. Comparison of wear of ultra-high molecular weight polyethylene acetabular cups against surface-engineered femoral heads. *Proc. Inst. Mech. Eng. H* **2008**, *222*, 1073–1080.
8. Xu, T.; Pruitt, L. Diamond-like carbon coatings for orthopaedic applications: An evaluation of tribological performance. *J. Mater. Sci.* **1999**, *10*, 83–90.
9. Dowling, D.; Kola, P.; Donnelly, K.; Kelly, T.; Brumitt, K.; Lloyd, L. Evaluation of diamond-like carbon-coated orthopaedic implants. *Diamond Relat. Mater.* **1997**, *6*, 390–393.
10. Platon, F.; Fournier, P.; Rouxel, S. Tribological behavior of DLC coatings compared to different materials used in hip joint prostheses. *Wear* **2001**, *250*, 227–236.
11. Kim, W.; Kin, J.; Park, S.; Lee, K. Tribological and electrochemical characteristics of DLC coatings with bias voltage. *Met. Mater. Intern.* **2005**, *11*, 473–480.

12. Shi, X. Hydrogenated diamond-like carbon film deposited on UHMWPE by RF-PECVD. *Appl. Surf. Sci.* **2009**, *255*, 246–251.
13. Puértolas, J.A.; Martínez-Nogués, V.; Martínez-Morlanes, M.; Mariscal, M.; Medel, F. Improved wear performance of ultra high molecular weight polyethylene coated with hydrogenated diamond like carbon. *Wear* **2010**, *269*, 458–465.
14. Sheeja, D.; Tay, B.; Nung, L. Tribological characterization of diamond-like carbon (DLC) coatings sliding against DLC coatings. *Diamond Relat. Mater.* **2003**, *12*, 1389–1395.
15. Takeno, T.; Sugawara, T.; Miki, H.; Takagi, T. Deposition of DLC film with adhesive W-DLC layer on stainless steel and its tribological properties. *Diamond Relat. Mater.* **2009**, *18*, 1023–1027.
16. Azzi, M.; Amirault, P.; Paquette, M.; Klemberg-Sapieha, J.E.; Martinu, L. Corrosion performance and mechanical stability of 316L/DLC coating system: Role of interlayers. *Surf. Coat. Technol.* **2010**, *204*, 3986–3994.
17. Trava-Airoldi, V.J.; Bonetti, L.F.; Capote, G.; Fernandes, J.A.; Blando, E.; Hübler, R.; Radi, P.A.; Santos, L.V.; Corat, E.J. DLC film properties obtained by a low cost and modified pulsed-DC discharge. *Thin Solid Films* **2007**, *516*, 272–276.
18. Yong, K.C.; Gang, S.K.; Kyoung, I.M.; Sang, G.K.; Sung, W.K. Tribological properties of the DLC films with different hydrogen content and Si addition. *Mater. Res. Soc. Symp. Proc.* **2005**, *903*, 114–119.
19. Chou, C.C.; Wu, Y.Y.; Lee, J.W.; Yeh, C.H.; Huang, J.C. Characterization and haemocompatibility of fluorinated DLC and Si interlayer on Ti6Al4V. *Surf. Coat. Technol.* **2013**, *231*, 418–422.
20. Chu, P.K.; Liu, C.L.; Yang, D.Z. *In vitro* evaluation of diamond-like carbon coatings with a Si/SiC<sub>x</sub> interlayer on surgical NiTi alloy. *Nucl. Instrum. Methods Phys. Res. B* **2007**, *257*, 132–135.
21. Choi, H.; Lee, K.R.; Park, S.J.; Wang, R.; Kim, J.G.; Oh, K.H. Effects of plastic strain of diamond-like carbon coated stainless steel on the corrosion behavior in simulated body fluid environment. *Surf. Coat. Technol.* **2008**, *202*, 2632–2637.
22. Yamauchi, N.; Ueda, N.; Okamoto, A.; Sone, T.; Tsujikawa, M.; Oki, S. DLC coating on Mg-Li alloy. *Surf. Coat. Technol.* **2007**, *201*, 4913–4918.
23. Erck, R.A.; Nichols, F.A.; Dierks, J.F. Pull-test adhesion measurements of diamond like carbon films on silicon carbide, silicon nitride, aluminum oxide, and zirconium oxide. *J. Vac. Sci. Technol. A* **1994**, *12*, 1583–1586.
24. Hoffmann, D.M.; Singh, B.; Thomas, J.H., III. *Handbook of Vacuum Science and Technology*, 3rd ed.; Academic Press: Waltham, MA, USA, 1998; pp.568.
25. Sasakim, Y.T. A survey of vacuum material cleaning procedures: A subcommittee report on the American Vacuum Society Recommended Practice Committee. *J. Vac. Sci. Technol. A* **1991**, *9*, doi:10.1116/1.577449.
26. *NanoSuite 5*; Agilent Technologies Inc: Waldbronn, Germany, 2013.
27. Oliver, W.C.; Pharr, G.M. Measurement of hardness and elastic modulus by instrumented indentation: Advances in understanding and refinements to methodology. *J. Mater. Res.* **2004**, *19*, 3–20.
28. Heeg, J.; Rosenberg, M.; Schwarz, C.; Barfels, T.; Wienecke, M. Optimised plasma enhanced chemical vapour deposition (PECVD) process for double layer diamond-like carbon (DLC) deposition on germanium substrates. *Vacuum* **2009**, *83*, 712–714.

29. Ward, L.P. Studies of Ion Plated Coatings for Biomedical Applications. Ph.D Thesis, University of Northumbria, UK, 1991.
30. Huang, L.; Xu, K.; Lu, J.; Guelorget, B.; Chen, H. Nano-scratch and fretting wear study of DLC coatings for biomedical application. *Diamond Relat. Mater.* **2001**, *10*, 1448–1456.
31. Poliakov, V.; Siqueira, M.; Veiga, W.; Hümmelgen, I.; Lepienski, C. Physical and tribological properties of hard amorphous DLC films deposited on different substrates. *Diamond Relat. Mater.* **2004**, *13*, 1511–1515.
32. Wu, J.B.; Chang, J.J.; Li, M.Y.; Leu, M.S.; Li, A.K. Characterization of diamond-like carbon coatings prepared by pulsed bias cathodic vacuum arc deposition. *Thin Solid Films* **2007**, *516*, 243–247.
33. Robertson, J. Diamond-like amorphous carbon. *Mater. Sci. Eng. R* **2002**, *37*, 129–281.

© 2014 by the authors; licensee MDPI, Basel, Switzerland. This article is an open access article distributed under the terms and conditions of the Creative Commons Attribution license (<http://creativecommons.org/licenses/by/3.0/>).